Magnetotransport and magnetization properties of p-type $Ga_{1-x}Mn_xAs$, a new III - V diluted magnetic semiconductor

1997 J. Phys.: Condens. Matter 9 L361

(http://iopscience.iop.org/0953-8984/9/24/003)

J. Phys.: Condens. Matter **9** (1997) L361–L367. Printed in the UK PII: S0953-8984(97)81083-1

LETTER TO THE EDITOR

Magnetotransport and magnetization properties of p-type $Ga_{1-x}Mn_xAs$, a new III–V diluted magnetic semiconductor

A Van Esch†‡, J De Boeck†, L Van Bockstal‡, R Bogaerts‡, F Herlach‡ and G Borghs†

† IMEC, Kapeldreef 75, B-3001 Leuven, Belgium

‡ Laboratorium voor Vaste-Stoffysica en Magnetisme, KU Leuven, B-3001 Leuven, Belgium

Received 20 January 1997, in final form 12 March 1997

Abstract. A new III–V diluted magnetic semiconductor (DMS), $Ga_{1-x}Mn_xAs$, can be grown by molecular beam epitaxy. When a low temperature growth procedure is followed, homogeneous material of excellent crystal quality with Mn concentrations up to $x \sim 9\%$ can be grown. Hole transport in these compounds is strongly affected by the antiferromagnetic exchange interaction between holes and Mn 3d spins. At a critical temperature T_c, with a value of around 50 K for Mn concentrations of 3–5%, magnetic long-range order of Mn–hole complexes induces a paramagnetic–ferromagnetic transition. Above T_c, it is shown that transport behaviour on both sides of the metal–insulator transition can be observed. Below T_c, due to the rising spontaneous magnetization, carrier mobility increases and the relative position of the Fermi level towards the mobility edge changes. Also, a negative magnetoresistance is measured.

Diluted magnetic semiconductors (DMSs) bridge the physics of magnetism and the physics of semiconductors. In particular the exchange interaction between the system of localized magnetic moments and delocalized bands drastically alters transport, optical and magnetic properties of the host semiconductor. The combination of the two is attractive for its interesting physics and possible new applications. The most common DMS materials are based on II–VI compounds doped with Mn, Co, Fe and Cr. A new class of III–V DMS compounds containing a large concentration of magnetic ions has recently drawn attention and the first successful growth of $In_{1-x}Mn_xAs$ by molecular beam epitaxy (MBE) was described a few years ago by Munekata *et al* [1].

Ohno *et al* investigated transport properties and observed a paramagnetic–ferromagnetic phase transition at 10 K in p-type $In_{1-x}Mn_xAs$ DMS materials [2]. They concluded that neither direct Mn–Mn interaction nor a Ruderman–Kittel–Kasuya–Yoshida (RKKY) interaction between Mn spins and delocalized carriers is responsible for the observed transport properties and ferromagnetic order. The mechanism responsible for the magnetotransport properties and the magnetic phase transition in $In_{1-x}Mn_xAs$ originates from the exchange interaction between the holes and Mn ions. We will show that the same mechanism is present in $Ga_{1-x}Mn_xAs$. We demonstrate that higher critical temperatures can be obtained because of the larger Mn concentrations that can be incorporated in the $Ga_{1-x}Mn_xAs$ compound when a low-temperature growth procedure is followed.

The electronic structure of a neutral Mn acceptor in GaAs, derived from electron-spin-resonance measurements, was described by Schneider *et al* [3]. In GaAs doped with Mn concentrations up to 5×10^{18} cm^{-3} [6] a manganese acceptor–hole complex (Mn–h) is formed by a hole in a delocalized $^4j_{3/2}$ orbit around the Mn ($3d^5$) acceptor core.

The ground state is formed by the antiferromagnetic coupling between the $S = \frac{5}{2}$ spin of the Mn core and the $j = \frac{3}{2}$ spin of the hole to form a Mn–h complex with $J = 1$ ($\boldsymbol{J} = \boldsymbol{S} + \boldsymbol{j}$) total angular momentum. The ground state energy is at 113 meV above the valence band and excited states with $J = 2$, 3 and 4 are formed at energies 2ε, 5ε and 9ε approaching the valence band, ε being the exchange coupling. The experimental values $2\varepsilon = 2.5 \pm 0.5$ meV and $g_{J=1} = 2.77$ are determined from EPR (electron paramagnetic resonance) [3] and susceptibility in combination with magnetization measurements [4]. The formation of a neutral Mn–h complex is comparable to that of a bound magnetic polaron [3] with one single localized magnetic moment. The Mn–h eigenstates and eigenvalues of a dilute system are altered when the Mn concentration is increased to $\sim 10^{20}$ cm^{-3}. In the heavily doped semiconductor the localized hole orbitals overlap and form an impurity band. Based on the energy levels of the Mn–h complex in the dilute semiconductor, in its ground state the impurity band will be antiferromagnetically coupled to the Mn centres.

In the past, the highest Mn concentrations incorporated in the GaAs host lattice were limited to 10^{18}–10^{19} cm^{-3}. When a growth procedure comparable to that of low-temperature (LT) GaAs is used the Mn concentration can be increased considerably [5] as the LT growth procedure suppresses surface segregation of Mn. After the growth of an LT GaAs buffer layer of typically 200 nm a Mn flux is supplied to grow $Ga_{1-x}Mn_xAs$. Typical conditions are the following: substrate temperature, 500–550 K; growth rate, 0.6–0.8 μm h^{-1}; beam equivalent pressures of Ga, 3.3×10^{-7} Torr, and As_4, 6×10^{-6} Torr. Samples up to 3 μm thick with Mn concentrations between 3 and 8% have been grown without any signs of quality loss. Annealing the samples leads to formation of As precipitates above ~670 K and to the formation of nanometre-scale magnetic MnAs particles at temperatures above 770 K. The size of the particles depends on the annealing temperature and Mn alloy concentration. These experiments are described in more detail elsewhere [5]. The alloy concentration of Mn is determined by the effusion flux and checked after growth by energy dispersive x-ray analyses. Structural characterization by high-resolution electron microscopy (HREM) [6] and x-ray diffraction spectrum linewidth measurements confirmed good crystal quality. $Ga_{1-x}Mn_xAs$ retains the zincblende crystal structure of GaAs and for low Mn concentration the lattice parameter obeys Vegard's law very closely, taking hypothetical zincblende MnAs and LT GaAs as references. The non-stoichiometric As concentration due to the LT growth makes Vegard's law inadequate for higher Mn concentrations (i.e. for $x \geqslant 8$–9%).

$Ga_{1-x}Mn_xAs$ films with Mn alloy concentrations up to 8% and a thickness of 0.4–2 μm were studied by magnetotransport and magnetization measurements. Hall resistivity ρ_{Hall} and resistivity ρ were measured from room temperature to 1.5 K and in magnetic fields up to 8 T. For the transport measurements, all samples were patterned into Hall bars. In order to change the magnetically and electronically active Mn content the films were also annealed between growth temperatures and 680 K. During the annealing treatment, the $Ga_{1-x}Mn_xAs$ layers were covered with a clean piece of GaAs to avoid As evaporation from the surface. A forming gas atmosphere suppresses oxidation. Although the precise mechanism of 'locking out' Mn spins is not yet known, in practice we can change the magnetization continuously and in a controlled way. From HREM on multilayered structures of $Ga_{1-x}Mn_xAs$–GaAs–AlAs it can be inferred that As atoms are much more mobile than Mn atoms and diffuse preferentially towards the Mn atoms to form Mn–As complexes. The formation of large Mn–As ferromagnetic particles has not been observed. If such particles were present, their size would have to be smaller than 1 nm and particles would be superparamagnetic over the whole temperature range as was clear from magnetization measurements on samples annealed at 770 K [5].

Below a transition temperature T_c dependent on the Mn concentration, the material

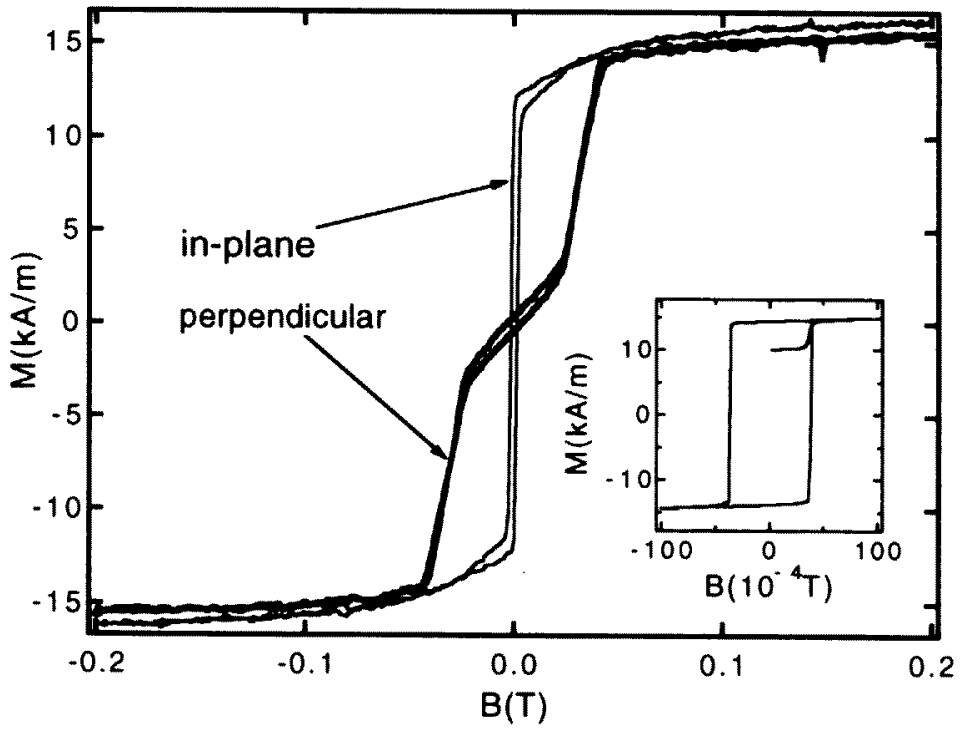

Figure 1. Perpendicular and in-plane magnetization of $Ga_{0.92}Mn_{0.08}As$ (M311) below T_c ($T = 10$ K). The inset shows SQUID magnetization measurements on $Ga_{0.93}Mn_{0.07}As$ (M279) at 4 K.

becomes ferromagnetic. An in-plane magnetization is measured with a very low coercive field as shown in figure 1, where both the perpendicular and parallel magnetization measurements are presented. A square hysteresis loop is observed with saturation magnetization up to 15 kA m^{-1} at 4 K (see the inset in figure 1). The coercive field parallel to the sample surface is 0.004 T (40 G) and 0.05 T (500 G) for the direction perpendicular to the surface. As demonstrated by Ohno *et al* [7] magnetization orientation is determined by strain, reverting direction from in plane to out of plane when strain is changed from compressive to tensile. In the frame of a single localized moment polaron this can be explained by the behaviour of the hole system. Under a planar compression the valence band degeneracy at $k = 0$ is lifted and the in-plane light-hole band will be the lowest in energy [8]. The energy values and eigenstates of the coupled Mn–h system and at the same time the orientation of the magnetization will be determined by the energy of the partial hole system.

The saturated magnetization measurements show a deviation from the concentrations determined by energy dispersive x-ray analysis. For $g_{J=1} = 2.77$ and total spin $J = 1$ [5] a magnetization $M = \mu_B g_{J=1} J N_{Mn}/V$ is obtained indicating about 40% magnetically active manganese acceptor–hole complexes (Mn-h) for the samples shown in figure 1. Isolated Mn spins with no nearest-neighbour Mn ions give a full contribution to the susceptibility while Mn–As complexes are 'locked out' [9]. T_c increases with Mn concentration only up to $x \sim 5\%$; excess incorporation of Mn only adds to the formation of Mn–As complexes

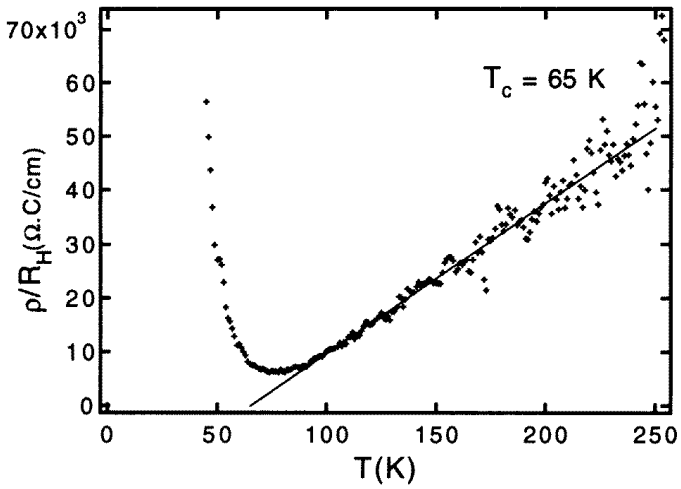

Figure 2. The dominant contribution of the extraordinary Hall effect to the Hall coefficient R_H is demonstrated by ρ/R_H being proportional to $(T - \theta_c)$. The above data are taken from $Ga_{0.94}Mn_{0.06}As$ (M271), annealed at 620 K.

which are not magnetically or electrically active, resulting in a lower net number of Mn–h complexes and consequently a decrease in T_c.

The Hall resistivity can be expressed as

$$\rho_{Hall} = R_0 B + R_s M \tag{1}$$

where R_o is the ordinary Hall coefficient, R_s the anomalous Hall coefficient, and M the magnetization of the film. With $M = \chi H$ and R_s proportional to ρ, above the Curie temperature θ_c equation (1) becomes

$$\rho_{Hall} = R_H B$$

with

$$R_H = R_o + c\rho\chi/\mu_0 \tag{2}$$

where c is a constant and μ_0 is the magnetic permeability of vacuum. Here, $B \approx \mu_0 H$ because of the thin-film demagnetization factor. In the paramagnetic region, the susceptibility χ is given by $C/(T - \theta_c)$. Figure 2 illustrates that the dominant contribution to the Hall coefficient originates from the extraordinary Hall effect: ρ/R_H is proportional to $(T - \theta_c)$ and R_o is zero within experimental error, preventing a determination of the number of charge carriers. Suggested by the resolution of the measurements the carrier concentration must be larger than $\sim 10^{18}$ cm^{-3}. θ_c was determined for different annealing temperatures; for all samples the Curie temperature θ_c is equal to the temperature T_c at which the local maximum in the resistivity curves occurs.

In contrast to weakly Mn doped GaAs, where activated transport behaviour with an activation energy of 113 meV is measured, no such exponential activation is present in our materials (shown in figure 3).

Above T_c, resistivity measurements show a transport behaviour characteristic for systems near the metal–insulator transition, the resistivity being inversely proportional to temperature. An expression for the conductivity above T_c can be derived from the

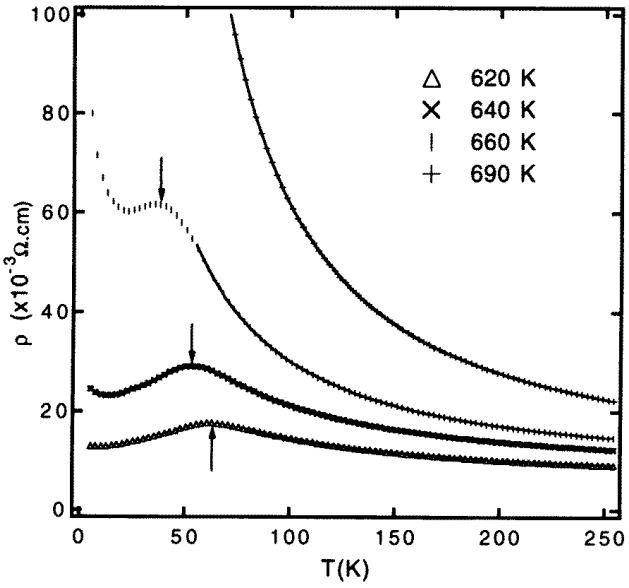

Figure 3. Resistivity measurements as a function of temperature on samples originating from $Ga_{0.94}Mn_{0.06}As$ (M271), subjected to the different annealing treatments indicated in the legend. The solid lines represent fits to equation (3).

calculations of Dubson and Holcomb [10] when scattering by phonons is included. This leads to

$$\rho(T) = \frac{C_1 + F}{kT \ln(\exp[(E_f - E_m)/kT] + 1)} \tag{3}$$

$$F = \frac{C_2}{\exp(\theta_D/T) - 1} \tag{4}$$

F represents phonon scattering and C_1 represents the temperature independent part. E_F is the Fermi level and E_m is the mobility edge, i.e. the energy level separating the localized from the extended states within the impurity band. C_2 is a constant. All fitted resistivity curves showed a Debye temperature θ_D close to 385 K in agreement with the phonon frequency in GaAs. Depending on the sign of $E_F - E_m$, the conductivity will tend to zero or stay finite as $T = 0$ K is approached, revealing insulating and metallic behaviour, respectively. From figure 4 it is evident that by lowering the active Mn content (either by changing the Mn effusion flux during growth or by post-growth annealing), $Ga_{1-x}Mn_xAs$ can be tuned through the metal–insulator transition. M311 (for all annealing treatments) and M271 annealed at 680 K are on the insulator side, M271 annealed at 660 K is exactly at the metal–insulator transition and all other samples are metallic. Assuming a constant density of states, a rough estimate of the carrier concentration can be made: $p \approx 3 \times 10^{19}$ cm^{-3} at $T = 100$ K and for $E_F - E_m = 0$. The annealing causes an increase in overall resistivity and a shift of T_c. Figure 4 illustrates that annealing reduces the number of Mn–h systems, changing both $E_F - E_m$ and the Curie temperature. This decrease in T_c as a function of annealing temperature is proof of an increased average distance between the magnetically active centres.

Below T_c the paramagnetic–ferromagnetic transition is initially accompanied by a decrease in resistivity as can be seen in figure 3. For sufficiently low temperatures the

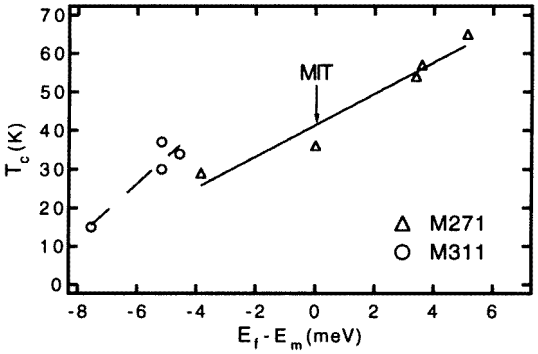

Figure 4. The Curie temperature versus the energy difference between the Fermi level and the mobility edge (obtained from fits as shown in figure 3) for different samples ($Ga_{0.92}Mn_{0.08}As$ (M311) and $Ga_{0.94}Mn_{0.06}As$ (M271)), each subjected to different annealing temperatures.

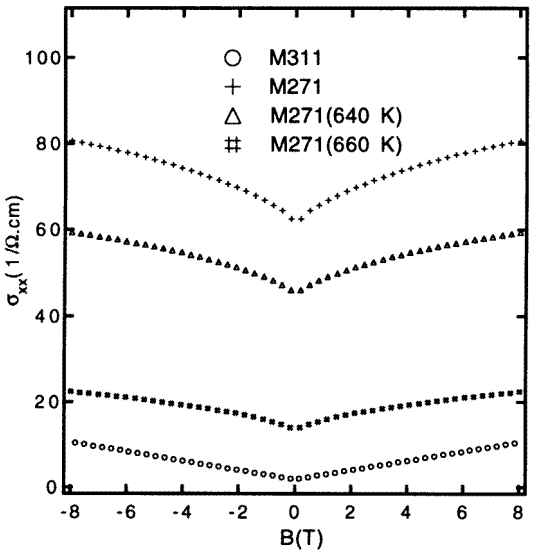

Figure 5. Magnetoconductivity of $Ga_{0.92}Mn_{0.08}As$ (M311) and of samples originating from $Ga_{0.94}Mn_{0.06}As$ (M271), subjected to the different annealing treatments indicated in the legend ($T = 10$ K).

resistivity again increases. This behaviour is the result of changes in both the mobility and the carrier concentration. The initial drop in resistivity below T_c is due to an increase in the carrier mobility, as is observed in ferromagnetic semiconductors [11]. For high carrier concentrations the spin disorder scattering remains constant in the paramagnetic region; below T_c it drops gradually until the magnetic order of the spin system is complete. As in traditional ferromagnetic semiconductors, the increasing magnetization causes a splitting of both the valence band and the impurity band. In conventional ferromagnetic semiconductors the splitting of the impurity band is always smaller than that of the valence band as the acceptor (or donor) level never originates from the magnetic element. Below T_c the activation energy decreases. This no longer holds for $Ga_{1-x}Mn_xAs$. On the contrary, the acceptor level is now strongly correlated to the magnetic centre. Hence, the energy $|E_F - E_m|$

required to excite a hole from the impurity band to a state above the mobility edge (in the valence band) increases as the magnetization increases. Below 10–20 K (depending on the Mn concentration) the magnetization has reached its saturation value and the mobility remains constant. The resistivity behaviour is now solely determined by the altered relative positions of E_F and E_m.

When an external field is applied, all Mn–h complexes align with the field; consequently the $j = \frac{3}{2}$ hole spins are forced anti-parallel with the field and their energy increases with the applied field. The Fermi level again moves towards the mobility edge. This is reflected in the negative magnetoresistance. In figure 5, the magnetoconductivity is shown for several samples.

In conclusion, by molecular beam epitaxy we have been able to grow $Ga_{1-x}Mn_xAs$—a new kind of III–V diluted magnetic semiconductor—with near-perfect crystal quality. A paramagnetic–ferromagnetic phase transition at critical temperatures around 50 K is observed in all samples ($x = 3$–9%), the critical temperature depending on the magnetically active Mn concentration. Resistivity measurements show that above the ordering temperature, materials on both sides of the metal–insulator transition can be fabricated. Below T_c, a strong interplay between magnetism and transport is observed. The effect of the rising spontaneous magnetization on the carrier mobility and Fermi level is qualitatively explained.

This work is supported by the Belgian Nationaal Fonds voor Wetenschappelijk onderzoek (BNFWO). The authors would like to thank B Grietens for providing the XRD measurements and G Verbanck for his help with the magnetotransport data. LVB and RB acknowledge the support of the BNFWO.

References

[1] Munekata H, Ohno H, von Molnár S, Segmüller A, Chang L L and Esaki L 1989 *Phys. Rev. Lett.* **63** 1849
[2] Ohno H, Munekata H, Penney T, von Molnár S and Chang L L 1992 *Phys. Rev. Lett.* **68** 2664
[3] Schneider J, Kaufmann J, Wilkening W and Baumler M 1987 *Phys. Rev. Lett.* **59** 240
[4] Frey Th, Maier M, Schneider J and Gehrke M 1988*J. Phys. C: Solid State Phys.* **21** 5539
[5] De Boeck J, Oesterholt R, Van Esch A, Bender H, Bruynseraede C, Van Hoof C and Borghs G 1996 *Appl. Phys. Lett.* **68** 2744
[6] Bender H, Van Esch A, Van Roy W, Oesterholt R, De Boeck J and Borghs G 1995 *Microsc. Sem. Mater. Conf. (Oxford) Inst. Phys. Conf. Ser. 146* (Bristol: Institute of Physics) p 293
[7] Ohno H, Shen A, Matsukura F, Oiwa A, Endo A, Katsumoto S and Iye Y 1996 *Appl. Phys. Lett*. **69** 363
[8] Osbourn G C 1985 *Superlatt. Microstruct.***1** 223
[9] Wolf P A 1988 *Semicond. Semimet.* **25** 413
[10] Dubson M A and Holcomb D F 1985 *Phys. Rev.* B **32** 1955
[11] Wallace P R, Harry R and Zuckermann M J 1973 *New Developments in Semiconductors* (Lijden: Noordhoff)